

Microscopic Monitoring of Local Temperature in the High Temperature Proton Exchange Membrane Fuel Cell Stack

Chi-Yuan Lee*, Fang-Bor Weng, Fan-Hsuan Liu, Chih-Ping Chang, Chih-Kai Cheng

Department of Mechanical Engineering, Yuan Ze Fuel Cell Center, Yuan Ze University, Taoyuan, Taiwan

*E-mail: cylee@saturn.yzu.edu.tw

Received: 12 September 2013 / Accepted: 3 October 2013 / Published: 20 October 2013

The non-uniform distributions of internal temperature in a membrane electrode assembly (MEA) of proton exchange membrane fuel cell (PEMFC) stack affect not only the reactions that occur in it, but also its performance and lifetime. In this work, micro-electro-mechanical systems (MEMS) are utilized to develop a new generation flexible micro temperature sensors for use in high-temperature electrochemical environments, and they were applied in high temperature fuel cell stack to measure the temperature. Polyimide foil (50 μ m) is selected as a substrate, and liquid polyimide is used as the protecting layer because of its high temperature resistance. The micro sensors were embedded in the cathode flow plate of HT-PEMFC stack (7 cells). The results demonstrate that they do not influence stack performance, and the calibration curves was measured by micro sensors are linearity and reliability. The curves of local temperature that were measured by micro sensors in the cell stack at the operating temperatures of 160°C and at constant currents of 2, 10 and 20A are fairly consistent each other. The results show that the non-uniform of heat distributions, and its internal chemical reaction is more severe, resulting in a large temperature difference inner HT-PEMFC stack at a constant current of 20A.

Keywords: MEMS, new generation flexible micro temperature sensors, polyimide, high temperature proton exchange membrane fuel cell stack

1. INTRODUCTION

The rapid development of technology industry causes climatic variation and energy crisis, so that various countries promote green energy industry actively, contributing to the rapid development of fuel cells and products.

In recent years, the application of fuel cells develops towards high temperature type gradually, as the low temperature fuel cell has the following problems, (1) the anode catalyst has CO poisoning in

low temperature ($<80^{\circ}\text{C}$) environment [1, 2]; (2) the present perfluorosulfonated film has good ionic conductivity only in high humidity environment; (3) the cathodic reduction potential is too high; (4) liquid water and heat removal [3].

The high temperature proton exchange membrane fuel cell is mixed with phosphoric polybenzimidazole (PBI) as membrane material, the operating temperature range is $120\sim 200^{\circ}\text{C}$, with the rise of operating temperature, the characteristics are (1) the CO poisoning at the anode can be reduced; (2) as the operating temperature exceeds 100°C , the gas humidification system for low temperature membrane is not required [4]; (3) over concentration of heat can be avoided, easy heat elimination; (4) it can be combined with reformer to produce hydrogen.

The high temperature fuel cell stack consists of multiple stacked single cells, in order to reach high performance, its internal local temperature is a very important parameter, too high temperature will influence the activity of the catalyst, dry membrane, mass transfer and heat management [5]; and too low temperature will result in incomplete reaction of membrane electrode assembly, so that the temperature distribution in the fuel cell stack is nonuniform [6-8]. Therefore, the heat management strategy for monitoring and discussing the internal temperature data and distribution of cell stack is very important.

Many previous studies discussed the efficiency and internal temperature data of fuel cell (stack), including (1) invasive; (2) external measurement; (3) simulation. Luke [9] used a self-made measuring plate to invade a high temperature fuel cell stack to measure the temperature, and compared it with simulation. Siegel [10] placed 36 resistance temperature detectors (RTD) on the cathode current collector plate of the high temperature fuel cell for external measurement, the experimental results showed there was significant temperature difference in different operating conditions of pure hydrogen and hydrogen (containing CO). Kurz [11] designed a high temperature fuel cell stack (5 cells) of open cathode, the performance curve and electrochemical impedance spectroscopy (EIS) measurement showed the power density was high, and the characteristic was similar to single fuel cell, the temperature differences among the fuel cells were small, the outside of bipolar plate was measured. Jung [12] designed a two-dimensional model of proton exchange membrane fuel cell, and simulated the temperature distribution in the membrane electrode assembly. However, the aforesaid methods have some problems, such as too large volume of detector, measurement inaccuracy, influencing the cell (stack) performance and unknown internal actual reactive state.

Ali [13] made TFTCs, embedded in high temperature fuel cell to measure the local temperature in reaction of internal membrane electrode assembly (MEA). Lee [14] used micro-electro-mechanical systems (MEMS) technology to develop micro temperature sensors, and embedded it in high temperature fuel cell stack (4 cells), the experimental results showed there was no influence on the performance of the fuel cell stack, and the temperature distribution was nonuniform.

Therefore, this study uses the MEMS technology to innovate a new generation flexible micro temperature sensor applicable to high temperature electrochemical environment, it is carried by flexible substrate of polyimide (PI) foil in thickness of $50\mu\text{m}$ instead of stainless steel foil [14]. This slight micro sensor is characterized by small volume and high sensitivity, it can be embedded in HT-PEMFC stack for temperature calibration without influencing the operation of fuel cell stack, implementing instant microscopic diagnosis and analysis, the performance of the fuel cell stack with

micro sensor is compared with that without micro sensor, and the local temperature variation and distribution in different cells in the fuel cell stack are monitored and discussed in different operating conditions.

2. SENSING PRINCIPLE OF MICRO TEMPERATURE SENSOR

The micro temperature sensor used in this study is the resistance temperature detector (RTD) with positive temperature resistance coefficient, the electrode form is serpentine structure, the sensing head area is $400 \times 400 \mu\text{m}$, and the minimum linewidth is $10 \mu\text{m}$, as shown in figure 1.

When the ambient temperature rises, due to the characteristic of positive temperature resistance coefficient, the resistance value of RTD increases accordingly. The relation between ambient temperature variation and the measured resistance variation is expressed as Eq. (1).

$$R_t = R_0(1 + \alpha_1 \Delta T) \quad (1)$$

where R_t is the resistance value (Ω) at $t^\circ\text{C}$, R_0 is the resistance value at reference temperature, and ΔT is the temperature difference ($^\circ\text{C}$) in relation to the reference temperature 0°C .

Eq. (1) can be changed to Eq. (2).

$$\alpha_1 = \frac{R_t - R_0}{R_0(\Delta T)} \quad (2)$$

where the physical meaning of α_1 is the sensitivity of micro sensor ($1/^\circ\text{C}$).

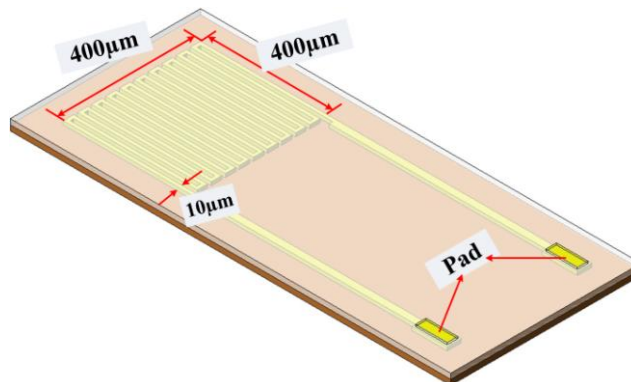


Figure 1. Schematic diagram of new generation flexible micro temperature sensor.

3. FABRICATION PROCESS

The past research had embedded a micro-temperature sensor in a proton exchange membrane fuel cell (PEMFC) to monitor temperature in the fuel cell, but the stainless steel foil based sensor's thermoresistance does not suit to high temperature electrochemical environment [14]. This study uses the process technology of MEMS to innovate a new generation flexible micro temperature sensor applicable to high temperature electrochemical environment, the substrate is flexible polyimide foil

(50µm), and the insulating and protective layers of the micro sensor are made of PI which has good temperature resistance.

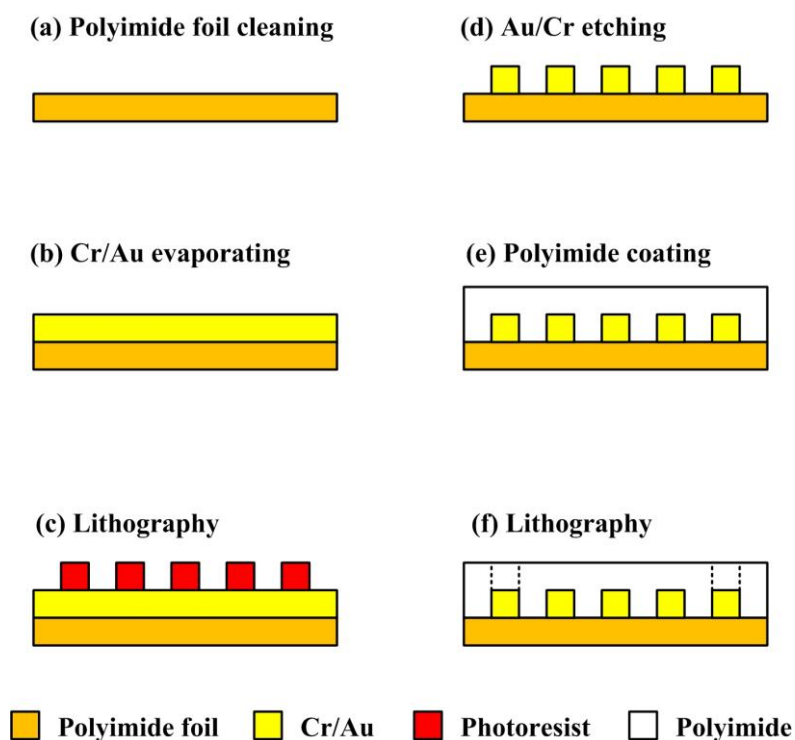


Figure 2. Process diagram of new generation flexible micro temperature sensor.

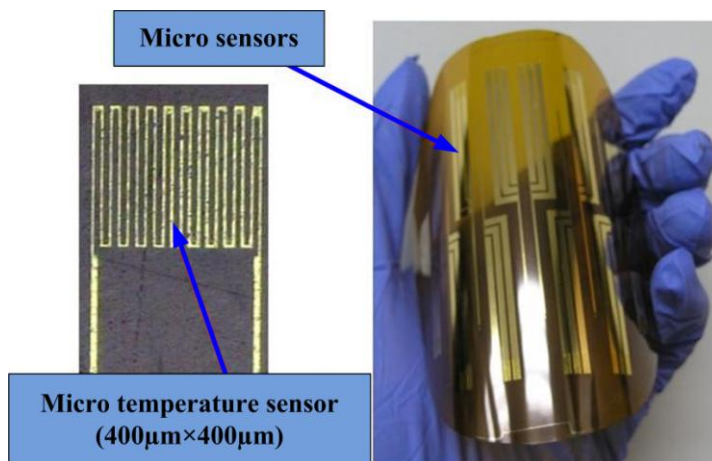


Figure 3. Real photo and optical micrograph of new generation flexible micro temperature sensor.

The fabrication process is shown in figure 2: (a) the PI foil is cleaned with acetone and methanol; (b) the E-beam evaporator is used to evaporation Cr as adhesion layer and Au as sensing layer; (c) the photolithography is used to define the temperature sensing pattern; (d) the temperature sensing pattern of micro sensor is etched by wet etching; (e) the spin coater is used to coat PI as the insulating and protective layer material of micro sensor; (f) the signal pad is exposed by using photolithography for continuous signal transfer and output.

Figure 3 shows the photo and optical microscope of the finished new generation flexible micro temperature sensor, this micro sensor is characterized by small volume, acid corrosion resistance, good temperature tolerance, quick response, real-time measurement, free placement and batch manufacturing.

4. CALIBRATION OF FLEXIBLE MICRO TEMPERATURE SENSOR

When the new generation flexible micro temperature sensor is made, the micro sensor is embedded in the cathode flow channel plate, facing to the membrane electrode assembly (MEA) and above the ribs of flow channel plate.

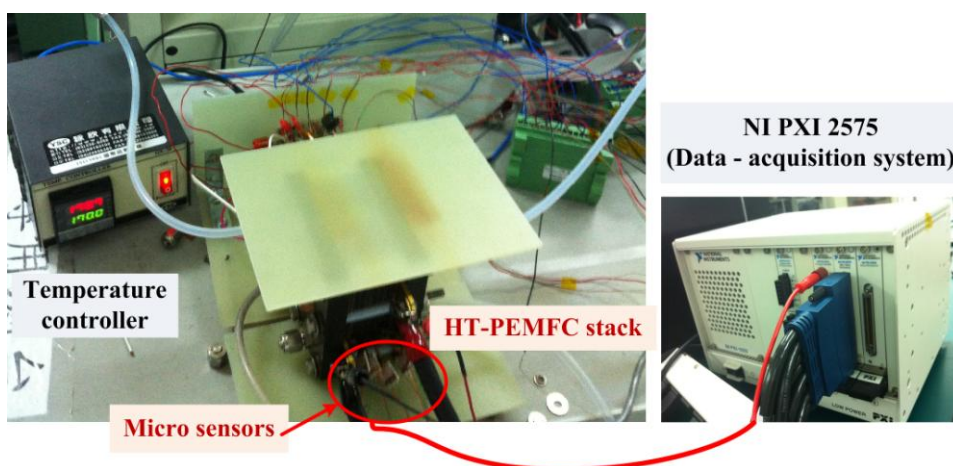


Figure 4. Calibrating instrument for micro temperature sensor.

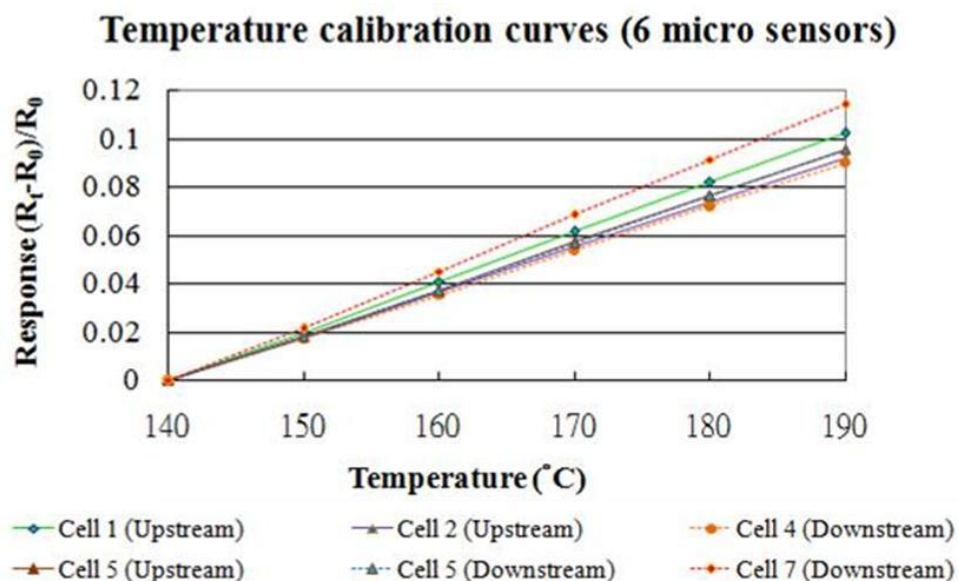


Figure 5. Temperature calibration curves of six micro sensors.

This study uses the temperature controller of external fuel cell stack directly as the calibration basis, so as to calibrate the temperature of micro sensor and to validate its reliability. The calibrating instrument is mounted as shown in figure 4. When the temperature is stable, the NI PXI 2575 data acquisition system is used to capture the resistance value of micro sensor. Figure 5 shows the calibration curves measured by the micro sensor embedded in high temperature fuel cell stack in the temperature range of 140°C to 190°C. Table 1 shows the linearity of micro temperature sensors, the results show that the micro temperature sensors have good linearity and reliability.

Table 1. Linearity of micro temperature sensors.

| Micro sensors | Linear trend (R^2) |
|---------------------|------------------------|
| Cell 1 (Upstream) | 0.9999 |
| Cell 2 (Upstream) | 0.9999 |
| Cell 4 (Downstream) | 0.9999 |
| Cell 5 (Upstream) | 0.9998 |
| Cell 5 (Downstream) | 0.9997 |
| Cell 7 (Downstream) | 0.9998 |

5. MICROSCOPIC PERFORMANCE DIAGNOSIS OF LOCAL TEMPERATURE IN HIGH TEMPERATURE FUEL CELL STACK

Table 2. Test conditions for high temperature fuel cell stack.

| Item | Condition |
|---|------------------|
| Fuel cell stack temperature (°C) | 160 |
| Flow rate at anode plate (H ₂) (slpm) | 4 |
| Flow rate at cathode plate (Air) (slpm) | 12 |
| Gas temperature | Room temperature |
| Rated current (A) | 2, 10, 20 |
| Reaction area (cm ²) | 31.4 |

In recent year, some researches still evaluate the thermal properties of polyimide in fuel cells by TGA [15], or using thermocouple to measure the temperature distribution in fuel cell stacks [16]. Then after the calibration of reliability test of micro temperature sensor, the high temperature fuel cell stack of 7 cells (including micro sensor) is tested. When the fuel cell stack temperature is 160°C, the anode and cathode plates are given different unhumidified gas flows, the performance curve of high temperature fuel cell stack with and without micro sensor is measured respectively, and the difference is analyzed; in the case of constant current (2, 10, 20A) for different loads, 30 minutes output. The

actual data and variation of local temperature in the fuel cell stack are obtained by instant and continuous measurement of NI PXI 2575 data acquisition system, the detailed operating conditions are shown in table 2. This experiment is carried out when the temperature and open circuit voltage (OCV) of fuel cell stack are stable.

5.1. Comparison between Performances of Fuel Cell Stacks with and without Embedded Micro Sensors

Figure 6 compares the performance curves of the high temperature fuel cell stack of 7 cells at 160°C with and without micro sensors, as the micro sensor embedded in the fuel cell stack covers the reaction area of MEA, blocking the gas from reacting with the covered MEA. According to table 3, as the micro sensors are in small size, the micro sensors embedded in the fuel cell stack will not influence the performance.

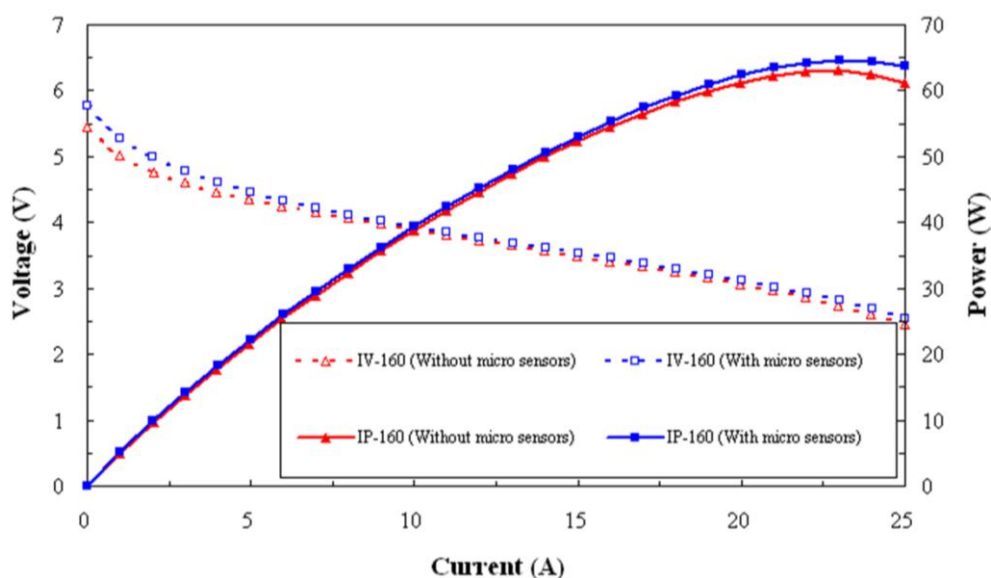


Figure 6. Comparison between performances of fuel cell stacks with and without embedded micro sensors.

Table 3. Reaction area and maximum power with and without micro sensors.

| | With micro sensors | Without micro sensors |
|----------------------------------|--------------------|-----------------------|
| Reaction area (cm ²) | 31.06, about 1% | 31.4 |
| Maximum power (W) | 64.6 (160°C) | 63.0 (160°C) |

5.2. Results of different currents (2, 10, 20A)

In the operating condition of 160°C, the measured local temperature information in fuel cell stack of different cells is discussed and analyzed as follows:

(1) Figure 7 shows the local temperature in different cells. It is observed that the temperature increases gradually with the rated current (2, 10, 20A), as the higher the operating current is, the higher is the heat released from chemical reaction, and in the case of high current (20A), the hot stack gets worse gradually.

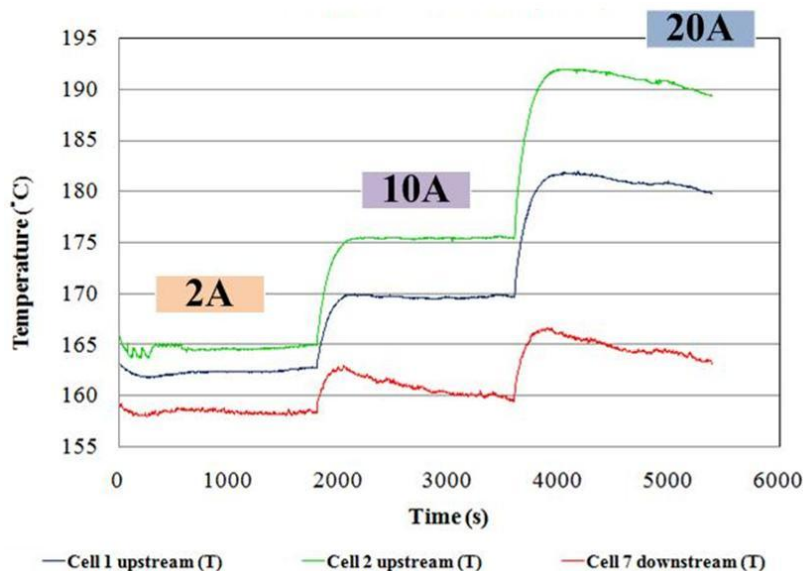


Figure 7. Local temperature in different cells (160°C).

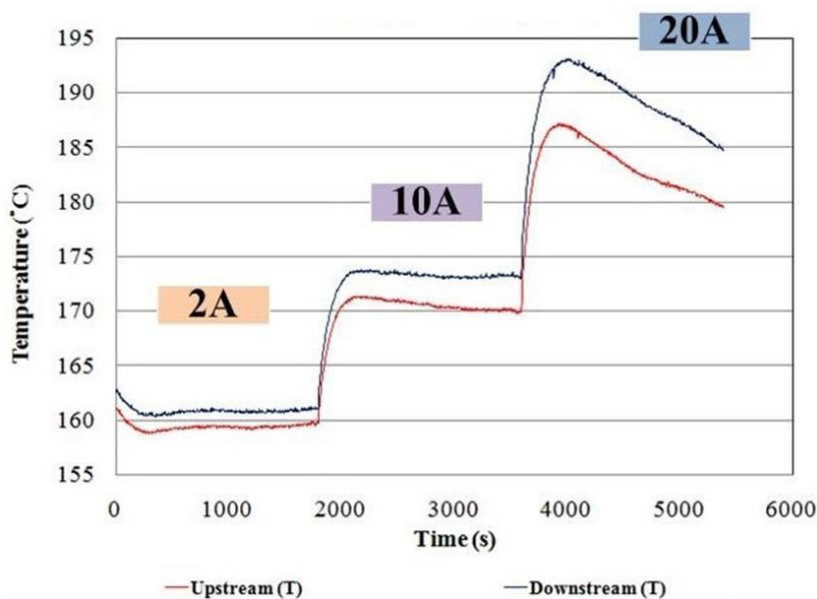


Figure 8. Local temperature in Cell 5 (160°C).

The temperature of Cell 7 is apparently lower than that of other cells, because the micro sensor is close to the metal collector plate, the thermal dispersion is fast, and the cathode plate flow rate is high, it is room temperature when the gas is led in, so that the temperature of Cell 7 is lower; the temperature of Cell 2 is higher, it may be because it is close to the anode plate, as well as at the end of cathode plate, the cathode plate gas takes the heat from the start to the end (Cell 7 to Cell 1). The internal chemical reaction is drastic in the case of high current (20A), and there is heat concentration.

(2) Figure 8 shows local temperature in Cell 5. The result shows the downstream temperature is higher than upstream, because the upstream is supplied with cold air continuously, so that a small amount of heat is taken away, the temperature is lower than the downstream end; the temperature gap increases gradually with the rated current, because the internal chemical reaction becomes drastic gradually, and the temperature distribution is nonuniform.

6. CONCLUSION

This study successfully used MEMS technology to develop new generation flexible micro temperature sensors applicable to high temperature electrochemical environment, its carrier substrate is polyimide foil in thickness of 50 μ m, the protective layer material is PI with better temperature tolerance, and the overall production process is simple. This new generation micro sensor has advantages of small size, acid corrosion resistance, good temperature tolerance, free placement, instant measurement and batch production.

In addition, this study embedded micro temperature sensors in the cathode flow field plate of fuel cell stack successfully, the temperature calibration curves of micro sensor are measured in the temperature range of 140°C to 190°C, the results show that the linearity and reliability are good. The comparison between performance curves with and without micro sensor shows the micro sensor embedded in the fuel cell stack has no effect on the performance. In the conditions of operating temperature 160°C and rated current (2, 10, 20A), the curvilinear tendencies of local temperature in the fuel cell stack measured by micro sensor are quite consistent, proving the reliability of micro sensor. The test results show that the heat distribution in the fuel cell stack is nonuniform, the temperature difference is large, and there is hot stack. In the operating condition of high current (20A), as the internal chemical reaction is drastic, the temperature difference between micro sensors is large.

ACKNOWLEDGEMENTS

This work was accomplished with much needed support and the authors would like to thank for the financial support by Bureau of Energy, Ministry of Economy Affairs of R.O.C. through grants 102-D0622 and National Science Council of R.O.C. through the grant NSC 102-2221-E-155-033-MY3 and NSC 102-2622-E-155-003. The authors also like to thank Shih Hung Chan and Ay Su of Yuan Ze University for their valuable advice and assistance in the experiments. In addition, we would like to thank the YZU Fuel Cell Center and NENS Common Lab, for providing access to their research facilities.

References

1. P. Krishnan, J. S. Park, C. S Kim; *J. Power Sources* 159 (2006) 817-823.

2. K. Kwon, D. Y. Yoo and J. O. Park; *J. Power Sources* 185 (2008) 202-206.
3. S. Bose, T. Kuila, T. X. H. Nguyen, N. H. Kim, K. T. Lau and J. H. Lee; *Prog. Polym. Sci.* 36 (2011) 813-843.
4. C. Yang, P. Costamagna, S. Srinivasan, J. Benziger and A. B. Bocarsly; *J. Power Sources* 103 (2001) 1-9.
5. J. L. Jespersen, E. Schaltz and S. K. Karb; *J. Power Sources* 191 (2009) 289-296.
6. X. Yuan, J. C. Sun, H. Wang and J. Zhang; *J. Power Sources* 161 (2006) 929-937.
7. K. P. Adzakpa, J. Ramousse, Y. Dube, H. Akremi, K. Agbossou, M. Dostie, A. Poulin and M. Fournier; *J. Power Sources* 179 (2008) 164-176.
8. M. Miller and A. Bazylak; *J. Power Sources* 196 (2011) 601-613.
9. L. Luke, H. Janßen, M. Kvesi, W. Lehnert and D. Stolten; *Int. J. Hydrogen Energ.* 37 (2012) 9171-9181.
10. C. Siegel, G. Bandlamudi and A. Heinzl; *Int. J. Hydrogen Energ.* 36 (2011) 12977-12990.
11. T. Kurz and J. Keller; *Fuel Cells* 4 (2011) 518-525.
12. C. Y. Jung, H. S. Shim, S. M. Koo, S. H. Lee and S. C. Yi; *Appl. Energ.* 93 (2012) 733-741.
13. S. T. Ali, J. Lebak, L. P. Nielsenc, C. Mathiasenc, P. Møller and S. K. Karb; *J. Power Sources* 195 (2010) 4835-4841.
14. C. Y. Lee, F. B. Weng, C. H. Cheng, H. R. Shiu, S. P. Jung, W. C. Chang, P. C. Chan, W. T. Chen and C. J. Lee; *J. Power Sources* 196 (2011) 228-234.
15. M. Lee, S. B. Khan, K. Akhtar, H. Han and J. Seo; *Int. J. Electrochem. Sci.* 8 (2013) 4225-4233.
16. J. Supra, H. Janßen, W. Lehnert and D. Stolten; *Int. J. Hydrogen Energ.* 38 (2013) 1943-1951.